ISSN: 2633-4828 Vol. 5 No.4, December, 2023

International Journal of Applied Engineering & Technology

FINITE ELEMENT ANALYSIS OF FEMUR BONE UNDER TRANSIENT LOADING CONDITIONS

Mayur Sunil Kharade* **and Richa Agrawal**
Pillai College of Engineering, New Panvel, Navi Mumbai, India
mayurkharade92@gmail.com and ragrawal@mes.ac.in

ABSTRACT
The present study is based on the use of a 3D simulation technique to determine the forces exerted on the femur bone during walking and further using it to carry out finite element analysis of femur bone. The simulation was done taking into consideration the effect of body weight, all thigh muscles and all contact forces at the hip, patella-femoral and knee joints. The results showed that the maximum forces were found between 0.75 sec (40%) and 0.95 sec (60%) of the posture phase, while the moments of highest twisting were immediately following heel strike. The study also found that muscle activity can reduce the internal loads on the femur bone by up to 24%. The findings of this study provide valuable insights into the forces exerted on the femur bone during walking. The obtained dynamic forces acting on the femur was further used to perform finite element analysis of the femur. The appropriate material selection and boundary conditions was used and the transient structural analysis was performed using ANSYS package. This approach resulted in more accurate results as compared to applying a static load depending on the body weight on the femur. The findings contribute to the understanding of femur loading dynamics and have implications for the development of interventions and treatments targeting femoral-related pathologies.

Keywords: Femur, Finite Element Analysis, Dynamic Loading

INTRODUCTION
Hip replacement surgery is a good option for short-term and mid-term pain relief. However, long-term results may be affected by complications such as aseptic loosening. Accurately determining the load applied to bone structure is crucial for developing precise and cost-effective metal implants [1]. Traditionally, the complex mechanical interaction between hard and soft tissue structures in the thigh has been treated as separate entities. The distribution of load in the femur is however significantly influenced by the interplay between muscles and bones, according to new studies [2]. The significance of the present work is as follows:

1. It provides valuable insights into load distribution patterns on the femur, which can be used to improve the design of hip replacement implants.
2. It helps to define the mechanical environment within the femur, which can be used to better understand the effects of hip replacement surgery on bone health.
3. It offers a basis for including additional physiological boundary constraints in experimental and numerical studies, which may result in a more accurate depiction of real-world scenarios.

Ultimately, this knowledge will aid in optimising surgical interventions and contribute to enhanced long-term outcomes for hip replacement procedures.

METHOD
The study focuses on analysing the mechanical environment of the femur under quasi-static conditions, assuming zero acceleration. It is assumed that the thigh and its constituent parts are in equilibrium at each time interval. Internal forces and moments define the static condition of the femur at each cross-section, which maintains equilibrium for all forces acting on the femur.

A free body analysis approach was employed to compute the femur's internal forces and moments. The study took into account the forces at the patella-femoral, hip, and knee points of contact, as well as the roles that muscles, ligaments, fasciae, compartments, and other soft tissue structures play in preserving equilibrium. The calculations

were based on the principle of equilibrium, ensuring that the forces and moments within the femur are balanced. By considering the interplay of various anatomical structures and external forces, a comprehensive understanding of the mechanical environment of the femur was achieved. The findings enhance our understanding of the complex interactions between different anatomical components, facilitating the development of more accurate models for biomechanical analyses. To calculate such forces the equilibrium Equ. 1 is used where Fm_i is 24 muscle forces, Fl_j is the ligament forces, G_k is the incremental force of thigh, Fc_{hip} is the hip contact force, $Fc_{patella}$ is the patella-femoral contact force and Fc_{knee} is the knee contact force.

$$\sum_i Fm_i + \sum_j Fl_j + G_k + Fc_{hip} + Fc_{patella} + Fc_{knee} = 0. \quad (1)$$

The muscle and ligament forces as per Gait analysis [3] which have been considered for the force calculations are tabulated in Table 1.

Table 1: Muscle Forces

Joint / Type	Muscle	Max Isometric Force (N)
HIP		
Right Hip Abdominal Muscle	glut_med_1	324
Right Hip Abdominal Muscle	glut_med_2	273
Right Hip Abdominal Muscle	glut_med_3	413
Right Hip Abdominal Muscle	glut_min_1	270
Right Hip Abdominal Muscle	glut_min_2	285
Right Hip Abdominal Muscle	glut_min_3	323
Right Hip Abdominal Muscle	glut_max_1	573
Right Hip Abdominal Muscle	glut_max_2	812
Right Hip Abdominal Muscle	glut_max_3	573
Right Hip Flexion	Adduction_Long_R	627
Right Hip Flexion	Adduction_Brev_R	429
Right Hip Flexion	Pubofemoral Ligament	266
Right Hip External rotation	Piriformis muscle1	381
Right Hip External rotation	Piriformis Muscle2	164
External rotation	Piriformis right	444
Right Hip External Muscle	Adductor_longus_1	381
Right Hip External Muscle	Adductor_longus_2	343
Right Hip External Muscle	Adductor_longus_3	488
Flexion Inner Rotation	iliacus	1073
Flexion, Inner Rotation	psoas	1113
HIP/KNEE		
Hip Flexion, knee External	Rectus femoris	1169
Hip Flexion, Hip Adduction, Knee Flexion	Gracilise Muscle	162
Hip Flexion, Hip Abduction, Knee Flexion	Sartorius Muscle	156
Hip Flexion, Hip Abduction, Hip Inner Rotation	Tensor Fasciae	233
Hip Extension, Hip Adduction, Knee Flexion	Semi Quadricep1	1288
Hip Extension, Hip Adduction	Semi Quadricep2	410
Hip Adduction, Knee Flexion	Semi Quadricep3	896
KNEE		
Extension	Vastus lateralis1	1294
Extension	Vastus lateralis2	1365

Extension	Vastus lateralis3	1871
Flexion	Biceps femorts	804
KNEE/ANKLE		
Knee Flexion, patellofemoral joint	Frontal Plantaris Muscle	1558
Knee Flexion, patellofemoral joint	Frontal Plantaris Muscle	683
ANKLE		
patellofemoral joint, Eversion	Posterior Calcaneofibular	435
patellofemoral joint, Eversion	Posterior Calcaneofibular long	943
patellofemoral joint	Soleus muscle	3549
patellofemoral joint, Inversion	Tibialis posterior	1588
patellofemoral joint, Inversion	Extensor hallucis longus tendon	310
	Extensor digitorum longus tendon	322
Dorsiflexion, Inversion	Peroneus tertius tendon	905
Dorsiflexion, Eversion	Extensor digitorum longus	512
Dorsiflexion, Inversion	Tibialis anterior m	162
Dorsiflexion, Eversion	Gastrocnemius m	180

The internal loads along a straight or curved path between the proximal and distal ends of the bone can be used to establish the internal loads acting along the long axis of the femur [4-5] provided muscle forces and courses of action are known. The forces mentioned in table 1 was used in Open-Sim simulation package to obtain the forces acting on the right hip and femur joint is as shown in Fig 1.

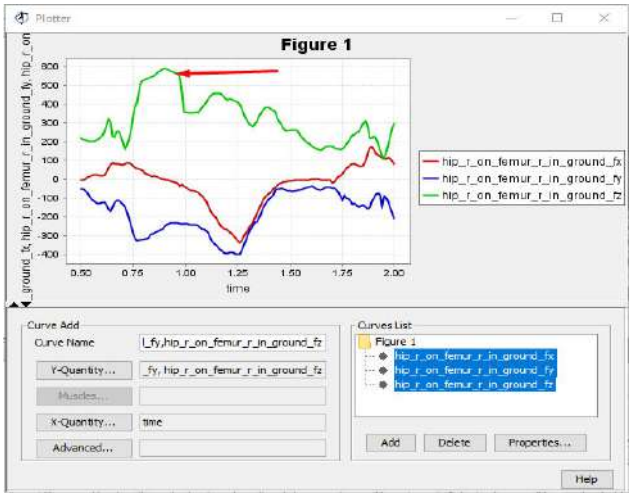

Figure 1: Forces on Femur

The internal loads, which were independent of the precise geometrical and material characteristics of the femoral cross-section, were the main focus of this investigation. Later continuum analysis was used to determine stresses and strains, allowing for a distinct evaluation of these elements. By determining internal weights along a long axis of the femur, this study provides valuable insights into the distribution of forces within the bone. These findings, combined with the muscle forces and lines of action, contribute to a more comprehensive understanding of the biomechanics of the femur. Furthermore, the availability of this data on Open-Sim Software enhances accessibility for researchers and clinicians, facilitating future studies and clinical applications in the field of femoral biomechanics.

This research lays the groundwork for subsequent continuum analysis to determine stresses and strains, enabling a deeper exploration of the mechanical behaviour of the femur. The outcomes of this study have the potential to inform the design and development of interventions and treatments for femoral-related conditions, ultimately improving patient outcomes and quality of life.

Model Considerations in Open-Sim. In the present study conducted using Open-Sim 4.4, certain model considerations were taken into account. Winter (1990) reported that the greater trochanter and femoral posterior cruciate ligament (PCL) insertion make up around 57% of the femur, which corresponds to the center of mass of the thigh [6]. To calculate the internal loads, the load distribution along the femur was thought to be linear. Therefore, based on this supposition, the center of mass of the proximal femoral part was calculated for each iteration of the internal load calculation. These modeling considerations align with the approach described by [7], providing consistency with previous research.

By incorporating these model considerations, this study aimed to enhance the accuracy of the internal load calculations and provide a more comprehensive understanding of the distribution of forces within the femur. The utilization of Open-Sim 4.4 facilitated the implementation of these model considerations and enabled the investigation of the biomechanical behavior of the femur.

The findings of this research contribute to the field of femoral biomechanics by providing insights into the distribution of forces within the femur and improving the understanding of the thigh's center of mass. This knowledge has implications for various applications, such as the development of personalized orthopedic interventions and the optimization of implant designs, ultimately leading to improved clinical outcomes and patient well-being.

Most muscle force vectors between the insertion and origin were shown as straight lines. Exceptions were the iliotibial band, wrapping around the greater trenchant, and the distal gluteus. In the present study, the model considered the insertion of the maxi mus muscle onto the femur. However, due to simplifications in the model [3] the wrapping of the iliopsoas and gastronomic muscles could not be taken into account. It should be noted that the inclusion of these muscle structures would provide a more comprehensive representation of the biomechanics of the thigh.

The model also incorporated the presence of the patella, which was represented by vector pairs of the vastus and rectus femoris muscles on one side and the patella r ligament on the other. This configuration allowed for the representation of the forces exerted by these muscle structures on the patella. Notably, according to study by George [8] additional contact points through the quadriceps muscles were taken into consideration and Flexion-ion angle was more than 80 degrees. These extra contact locations and the forces they produce were calculated and added as supplementary vector pairs to the internal load calculation model. This approach aimed to improve the accuracy of the internal load calculations by incorporating the relevant muscle forces and their interactions within the knee joint. Although certain simplifications were made, efforts were made to account for important muscle structures and their effects on the overall biomechanics of the thigh and knee joint.

These model considerations contribute to the scientific and methodological rigor of the study, allowing for a more accurate representation of the internal loads acting on the femur. Such detailed analyses are crucial for advancing our knowledge of the complex interactions between muscles, ligaments, and bone structures in the lower extremities and can inform the development of improved treatment strategies and orthopedic interventions. Maximum force we found when left foot is not in contact with floor as shown in Fig. 2. Figure 3 represent the forces acting on the femur in all three directions for a Gait cycle of right leg. The same is tabulated in Table 2.

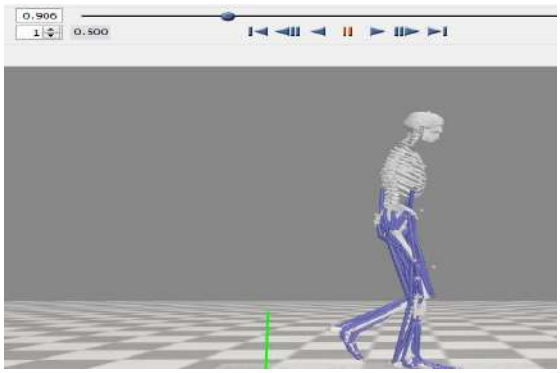

Figure 2: Exoskeleton Simulation

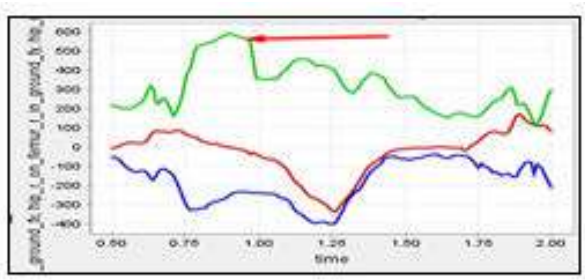

Figure 3: Open-Sim Graph

Table 2: Forces on Femur obtain from Open-Sim

Time (s)	F_x	F_z	F_y
0.5	-6.212489939	217.0288001	-56.06520159
0.55	19.25218605	197.2349991	-105.8633544
0.6	17.84129537	231.5360676	-124.5184282
0.65	82.00743277	225.4804697	-149.048343
0.7	75.45006974	194.9136507	-135.471724
0.75	69.5555617	329.0311211	-287.4256934
0.8	32.84448856	527.0029731	-321.8200506
0.85	16.19338981	552.5447504	-289.0854658
0.9	-2.305951157	590.3111328	-255.5967194
0.95	-16.96146574	564.8876546	-233.6853604
1	-46.91056613	354.5168787	-237.9119818
1.05	-69.31127176	354.7954003	-245.6268415
1.1	-123.2555684	406.9534014	-276.2019432
1.15	-222.2014035	455.5905538	-360.5200894
1.2	-274.3904464	414.9777871	-395.526631
1.25	-332.4194131	408.9113289	-403.7178254
1.3	-272.5680285	300.6698088	-297.4752115
1.35	-158.6542261	334.6198748	-207.1680267
1.4	-76.89503534	379.7103892	-107.9502373
1.45	-26.50279834	300.9990819	-52.27114139
1.5	-10.82487365	259.7289772	-65.20957711
1.55	-7.139989452	227.8522019	-59.04085705

1.6	-3.645752506	180.4792121	-41.70895102
1.65	-4.913693131	151.9484816	-59.12216398
1.7	-22.00789252	175.2986293	-47.28064961
1.75	26.10478724	160.2387489	-111.9044932
1.8	78.14766483	232.5403356	-136.5471999
1.85	70.87929501	294.1600835	-142.0030588
1.9	156.3092781	226.3640555	-100.2983168
1.95	109.4766124	109.8435343	-91.99223455
1.999	80.01420274	293.3135624	-211.8044721

Finite Element Analysis of Femur

Finite Element simulation of the femur bone was carried out using ANSYS package to gain insights into the mechanical behaviour of the femur under static and dynamic loading conditions. This model can be used to advance orthopedic research and clinical applications. The various stages are explained below.

Generation of 3D Model. A finite element model of the femur was developed using a series of software tools. First 3D Slicer was used to visualize the DICAOM images obtained from a CT Scan. The femur from segmented and the model was exported in STL format. Auto-desk Inventor 360 was used to refine the model by reducing the number of faces and smoothing the corners. The model was then exported in STEP format for further analysis. ANSYS Space-Claim was used to process and prepare the model for finite element analysis by meshing the model.

Material Model. A large number of literatures were studies to finalize the material properties for the analysis as it plays a major role for the finite element simulation. After a rigorous study [9-29] the material properties were finalized as mentioned in Table 3 and material model was created.

Table 3: Material Properties of femur Bone

Property	Value	Units
Density	950	kg/m^3
Coefficient of thermal expansion	$2x10^{-6}$	K^{-1}
Reference Temperature	25°	Degree
Young's Modulus	254	MPa
Poisson ratio	0.4	
Tensile Yield Strength	35	MPa
Compressive Yield Strength	145	MPa
Tensile Ultimate Strength	40	MPa
Compressive Ultimate Strength	149	MPa

Meshing. Static and Transient Structural Analysis was performed on the developed 3D model in ANSYS Workbench. The model was fine messed. The statistic of the messed model is mentioned in Table 4. Figure 4 shows the messed geometry.

Table 4: Meshing Statistics

	Values	Advance size functions	Relevance center	Span Angle
no of nodes	63452	On Proximity and Curvature	Fine	Fine
no of elements	40386			

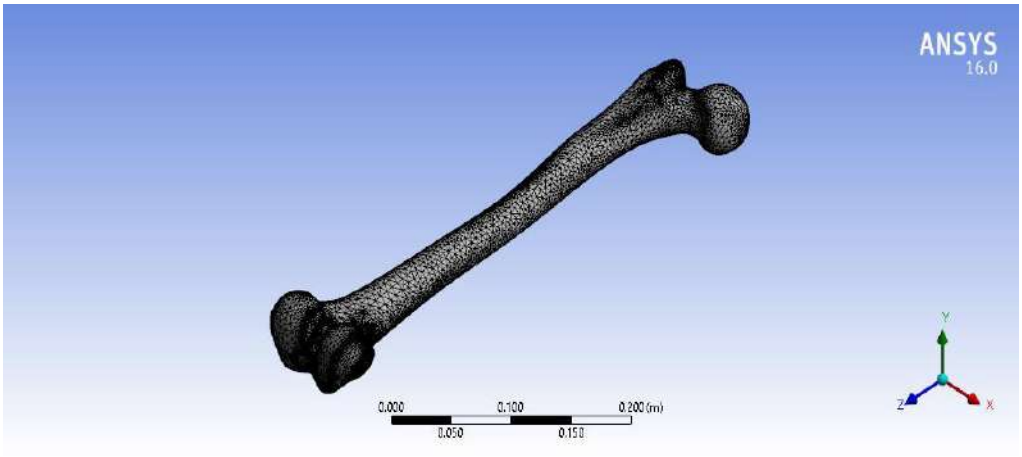

Figure 4: Meshed Model

Boundary Conditions. All forces as mentioned in table 2 obtained from Open-Sim Software were imported in tabular form of transient analysis module. Appropriate boundary conditions as shown in Fig. 5 that represent the constraints or supports of the structure were applied. These conditions include fixed constraints, and forces.

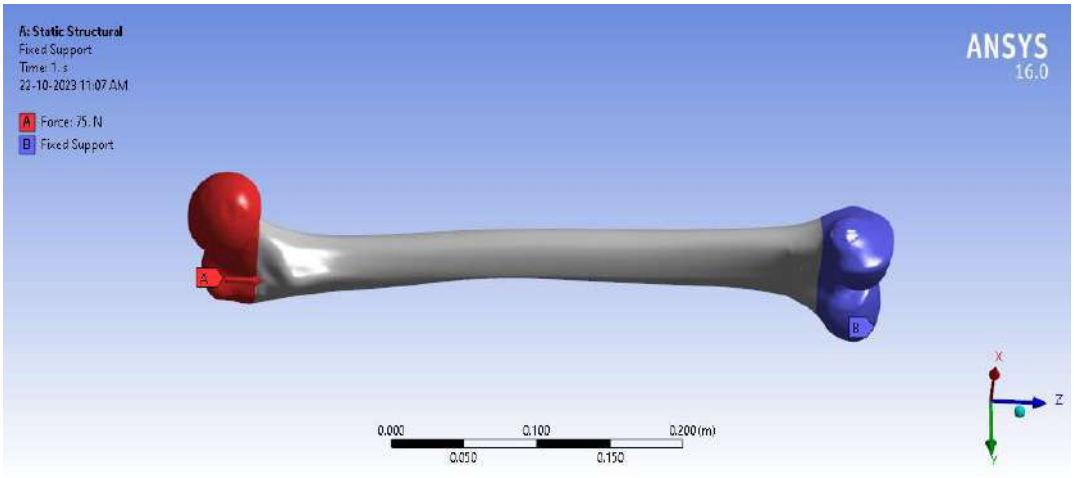

Figure 5: Boundary Conditions

Solution Setting. Time increment needs to be defined for the transient analysis. This determines how finely the time domain is divided and affects the accuracy and stability of the simulation. A smaller time step provides more accurate results but increases computational time. The same analysis was done by now considering static loading [30-31] in place of dynamic loads keeping all other parameters same.

RESULTS

The total deformation and equivalent stresses in the femur bone were calculated under both static and dynamic loading conditions. The results obtained are tabulated in Table 4.

Table 4: Results

Analysis	Total Deformation (mm)	Equivalent Stresses (MPa)
Static	1.1923	8.185
Transient	0.0119806	24.225

The total deformation for static and transient analysis is represented in Fig. 6 and Fig. 7. Similarly the equivalent stresses for static and transient analysis are represented in Fig. 8 and Fig. 9.

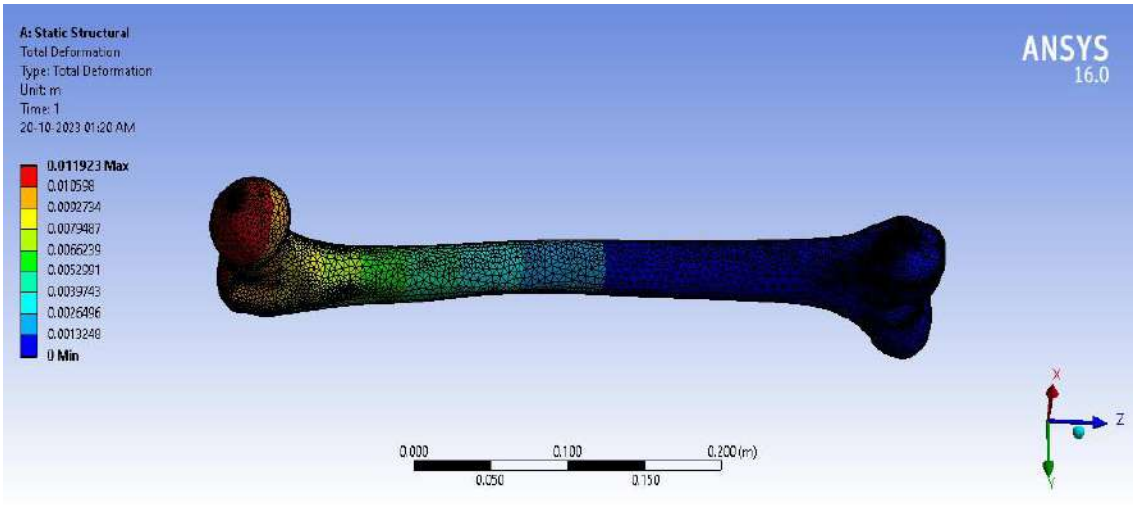

Fig 6: Total Deformation (Static)

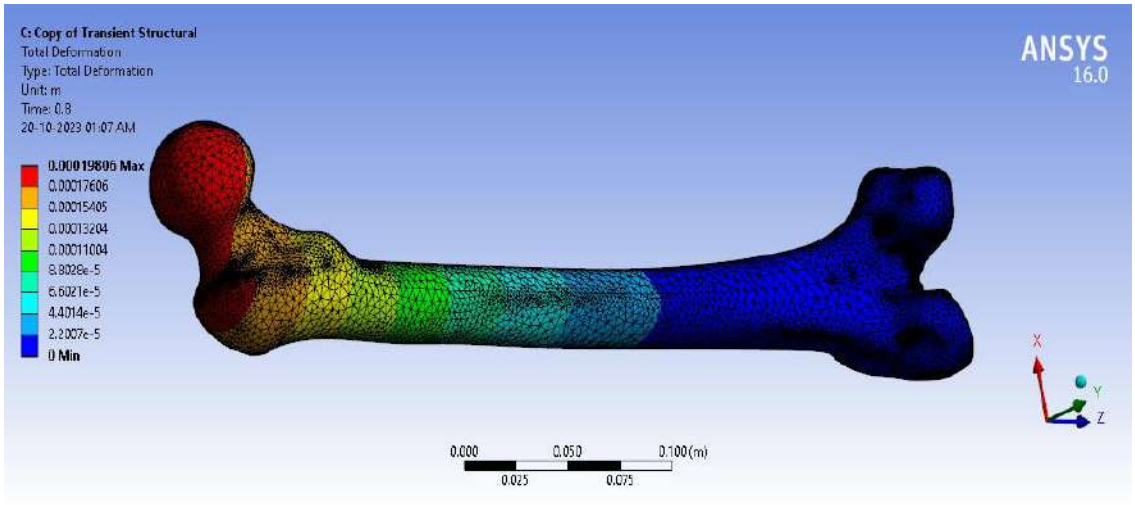

Fig 7: Total Deformation (Transient)

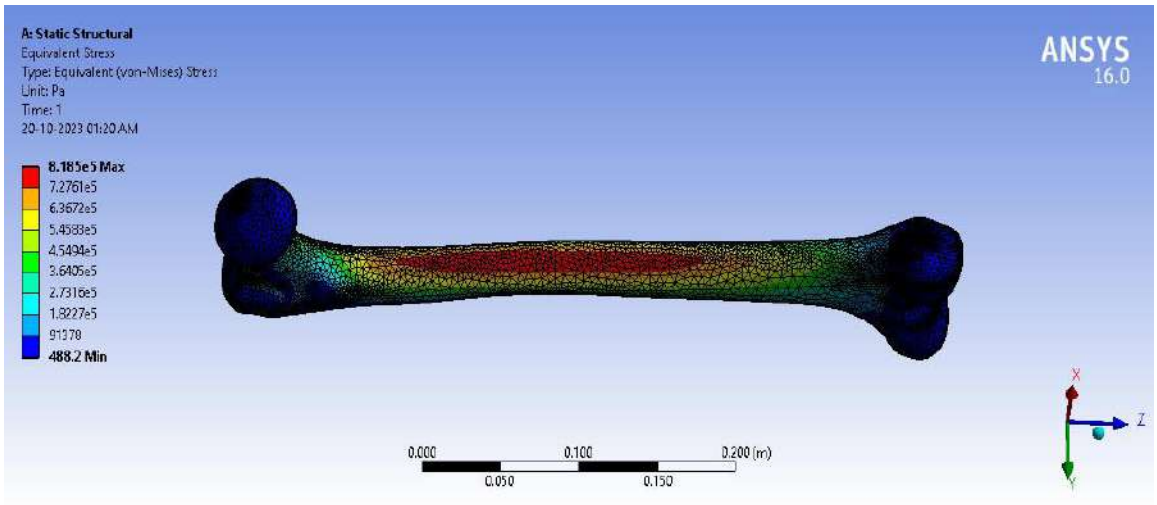

Fig 8: Equivalent Stresses (Static)

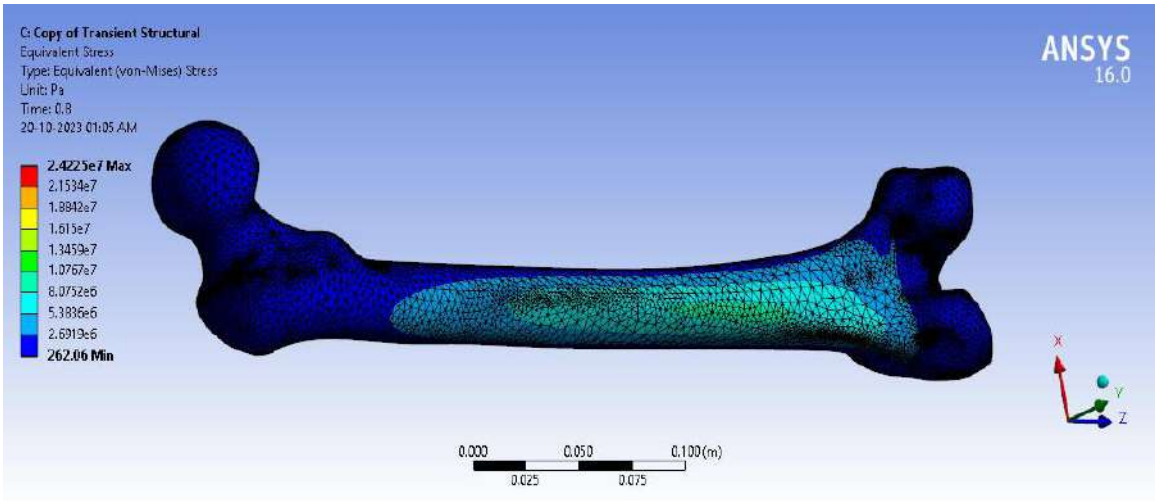

Fig 9. Equivalent Stresses (Transient)

CONCLUSION

To the best of the authors knowledge and review of previous research papers [30-35], it was discovered that transient load analysis on the femur bone has not been conducted. Most studies have focused on analyzing the femur bone by considering only the human body weight and applying a single directional force. Hence the present study shows that the stress on the femur is less under dynamic loading condition as compared to static loading condition. This is true as mentioned earlier the muscles absorbs 24% of the impact load while walking.

REFERENCES

[1] Abu-Amer, Y., Darwech, I., & Clohisy, J. C. (2007). Aseptic loosening of total joint replacements: mechanisms underlying osteolysis and potential therapies. *Arthritis research & therapy*, *9 Suppl 1*(Suppl 1), S6. https://doi.org/10.1186/ar2170

[2] Yang, S. I., Kim, K.-H., Kang, D., & Joo, S.-W. (2009). Cis-to-trans photoconversion of azobenzene self-assembled monolayers on gold nanoparticle surfaces investigated by Raman spectroscopy. Photochemical & Photobiological Sciences: Official Journal of the European Photochemistry Association and the European Society for Photobiology, 8(1), 31–33. doi:10.1039/b808903e

[3] Bergmann, G., Graichen, F., & Rohlmann, A. (1993). Hip joint loading during walking and running, measured in two patients. *Journal of biomechanics*, *26*(8), 969–990. https://doi.org/10.1016/0021-9290(93)90058-m

[4] Brand, R. A., Crowninshield, R. D., Wittstock, C. E., Pedersen, D. R., Clark, C. R., & van Krieken, F. M. (1982). A model of lower extremity muscular anatomy. *Journal of biomechanical engineering*, *104*(4), 304–310. https://doi.org/10.1115/1.3138363\

[5] Brand, R. A., Pedersen, D. R., & Friederich, J. A. (1986). The sensitivity of muscle force predictions to changes in physiologic cross-sectional area. *Journal of biomechanics*, *19*(8), 589–596. https://doi.org/10.1016/0021-9290(86)90164-8

[6] Gleeson, C., Hay, D. A., Johnston, C. J., & Theobald, T. M. (1990). "Twins in school". An Australia-wide program. *Acta geneticae medicae et gemellologiae*, *39*(2), 231–244. https://doi.org/10.1017/s0001566000005468

[7] Blankevoort, L. (1991). Passive motion characteristic of the human knee joint experiments and computer simulation. *Thesis, University of Nijmegon*.

[8] Duda, G. N., Schneider, E., & Chao, E. Y. (1997). Internal forces and moments in the femur during walking. *Journal of biomechanics*, *30*(9), 933–941. https://doi.org/10.1016/s0021-9290(97)00057-2

[9] B Lawrence Riggs, L Joseph Melton III,Richard A Robb. Population-Based Study of Age and Sex Differences in Bone Volumetric Density, Size, Geometry, and Structure at Different Skeletal Sites https://doi.org/10.1359/jbmr.040916

[10] M. Peacock, K.A. Buckwalter, S.Persohn (2009) . Race and sex differences in bone mineral density and geometry at the femur https://doi.org/10.1016/j.bone.2009.04.236

[11] Tony M Keaveny, David L Kopperdahl (2010) . Age-dependence of femoral strength in white women and men. https://doi.org/10.1359/jbmr.091033

[12] Ranu H. S. (1987). The thermal properties of human cortical bone: an in vitro study. *Engineering in medicine*, *16*(3), 175–176. https://doi.org/10.1243/emed_jour_1987_016_036_02.

[13] Lotz, J. C., Gerhart, T. N., & Hayes, W. C. (1990). Mechanical properties of trabecular bone from the proximal femur: a quantitative CT study. *Journal of computer assisted tomography*, *14*(1), 107–114. https://doi.org/10.1097/00004728-199001000-00020.

[14] Jae Young Rho, Richard B. Ashman (1993) .Young's modulus of trabecular and cortical bone material: Ultrasonic and micro tensile measurements. https://doi.org/10.1016/0021-9290(93)90042-D

[15] Sangbaek Park, S. Chae, (2013) Finite element modeling to estimate the apparent material properties of trabecular bone DOI:10.1007/s12541-013-0199-3

[16] T. Ueland, L. Stilgren, J. Bollerslev (2019). Bone Matrix Levels of Dickkopf and Sclerostin are Positively Correlated with Bone Mass and Strength in Postmenopausal Osteoporosis DOI:10.3390/ijms20122896

[17] Y. Emes, M. Ipekoğlu, Sabri Altintaş (2011) . The effects of freeze drying and solvent dehydration on the bending strength and calcium content of cortical bone. DOI:10.3944/AOTT.2011.2369

[18] Liliana Rincón-Kohli, P. Zysset (2009). Multi-axial mechanical properties of human trabecular bone. DOI:10.1007/s10237-008-0128-z

[19] A. Nazarian (2008). Relative interaction of material and structure in normal and pathological bone DOI:10.3929/ethz-a-005679110

[20] Janna M. Andronowski, M. E. Cole (2022). A multimodal 3D imaging approach of pore networks in the human femur to assess age-associated vascular expansion and Lacuno-Canalicular reduction. DOI:10.1002/ar.25089

[21] Diplesh Gautam, Venkatesh K. P. Rao (2021). Nondestructive Evaluation of Mechanical Properties of Femur Bone. DOI:10.1007/s10921-021-00754-0

[22] R. Voide, G. V. van Lenthe, R. Müller (2008). Differential Effects of Bone Structural and Material Properties on Bone Competence in C57BL/6 and C3H/He Inbred Strains of Mice. DOI:10.1007/s00223-008-9120-y

[23] C. Fölsch, Julian Dharma (2020). Influence of thermodis-infection on micro structure of human femoral heads: duration of heat exposition and compressive strength. DOI:10.1007/s10561-020-09832-5

[24] Dragomir-Daescu, D., Salas, C., Uthamaraj, S., & Rossman, T. (2015). Quantitative computed tomography-based finite element analysis predictions of femoral strength and stiffness depend on computed tomography settings. Journal of biomechanics, 48(1), 153–161. https://doi.org/10.1016/j.jbiomech.2014.09.016.

[25] Mirzaali, MJ, Schwiedrzik, J, Thaiwichai, S, Best, JP, Michler, J, Zysset, PK & Wolfram, U 2016, 'Mechanical properties of cortical bone and their relationships with age, gender, composition and microindentation properties in the elderly', Bone, vol. 93, pp. 196-211. https://doi.org/10.1016/j.bone.2015.11.018.

[26] Bayraktar, H. H., Morgan, E. F., Niebur, G. L., Morris, G. E., Wong, E. K., & Keaveny, T. M. (2004). Comparison of the elastic and yield properties of human femoral trabecular and cortical bone tissue. *Journal of biomechanics*, *37*(1), 27–35. https://doi.org/10.1016/s0021-9290(03)00257-4

[27] Lipson, S. F., & Katz, J. L. (1984). The relationship between elastic properties and microstructure of bovine cortical bone. *Journal of biomechanics*, *17*(4), 231–240. https://doi.org/10.1016/0021-9290(84)90134-9.

[28] Walsh, W. R., & Guzelsu, N. (1994). Compressive properties of cortical bone: mineral-organic interfacial bonding. *Biomaterials*, *15*(2), 137–145. https://doi.org/10.1016/0142-9612(94)90263-1

[29] Alejandro López, G. Mestres (2014). Compressive mechanical properties and cytocompatibility of bone-compliant, linoleic acid-modified bone cement in a bovine model.DOI:10.1016/j.jmbbm.2014.01.002

[30] Thasneem Fathima. (2020). Finite Element Analysis of Stress in Femur Bone. *International Journal of Progressive Research in Science and Engineering*, *1*(2), 25–32. Retrieved from https://journal.ijprse.com/index.php/ijprse/article/view/19

[31] Dey, S. K., Mainali, V., Pradhan, B. B., & Samanta, S. (2017). Numerical Stress Analysis of Artificial Femur Bone. In Advances in Systems, Control and Automation (pp. 139–155). Springer Singapore. https://doi.org/10.1007/978-981-10-4762-6_14

[32] Dhanopia, A., & Bhargava, M. (2017). Finite Element Analysis of Human Fractured Femur Bone Implantation with PMMA Thermoplastic Prosthetic Plate. In Procedia Engineering (Vol. 173, pp. 1658–1665). Elsevier BV. https://doi.org/10.1016/j.proeng.2016.12.190

[33] Seyedeh Fatemeh Shams, A. Mehdizadeh (2022). The comparison of stress and strain between custom-designed bone plates (CDBP) and locking compression plate (LCP) for distal femur fracture. DOI:10.1007/s00590-021-03160-4

[34] Muhammad Shahzad Masood, Atique Ahmad, R. Mufti (2013). Unconventional Modelling and Stress Analysis of Femur Bone under Different Boundary Condition (2017). Corpus ID: 111358883

[35] Aghili, A. L., Hojjati, M. H., Goudarzi, A. M., Rabiee, M., Aslan, M. H., Oral, A. Y., Özer, M., & Çaglar, S. H. (2011). Stress Analysis of Human Femur under Different Loadings. In AIP Conference Proceedings. *International Conference on Advances In Applied Physics And Materials Science. Aip*. https://doi.org/10.1063/1.3663174